

## Optical properties of nanostructured TiO<sub>2</sub> thin films

M Ben Karoui<sup>1</sup>, Z Kaddachi<sup>2</sup> and R Gharbi<sup>2</sup>

<sup>1</sup>. Laboratoire de Photovoltaïque, Centre de Recherche et des Technologies de l'Energie, Technopole de Borej-Cedria, BP 95, Hammam-Lif, Tunis. 2050, Tunisia.

<sup>2</sup>. LSDE-C3S. Ecole Nationale Supérieure d'Ingénieurs de Tunis. Université de Tunis, 05 Av. Taha Hussein 1008 Montfleury. Tunis, Tunisia.

E-mail: moufida\_gharbi@yahoo.fr

**Abstract.** Nanostructured titanium dioxide (TiO<sub>2</sub>) thin films were prepared with one and two layers on glass substrates (ITO) using sol gel-spin coating technique and annealed at temperature ranging from 300°C to 600°C. X-ray diffraction (XRD) and UV-Vis transmittance spectroscopy were used to study the effects of annealing temperature on the structural and optical properties. X-ray diffraction studies showed that the as-deposited films were amorphous and at first changed to anatase phase with increase of annealing temperature. Optical constants of these films were derived from the transmission and reflection spectra subjected to annealing at different temperatures. The results indicate that an anatase phase structure TiO<sub>2</sub> thin film with nanocrystallite size of about 10.72 nm can be observed at 400°C. The optical gap decreases from 3.82 eV to 3.74.eV for one layer and from 3.64 eV to 3.5 eV for two layers when the annealing temperature increases from 300 °C to 600°C. The refractive index is low compared to a pore free anatase TiO<sub>2</sub> and it increases contrary to the porosity which is reduced with the raising of the annealing temperature.

### 1. Introduction

TiO<sub>2</sub> thin films have specific characteristics such as the chemical stability, the non-toxicity, a high refractive index and a good transmittance in the visible region associated with a strong absorption in the ultraviolet. These properties allow their use in many applications: Optical components [1], ultraviolet attenuating agents for sunscreen cosmetic applications [2], optoelectronic sensors, photocatalyst [3,4]. They are also a good candidate for the fabrication of the dye sensitized solar cells DSSC [5].

Titanium dioxide is an excellent semi-conductor which crystallizes in three different crystalline structures: anatase (tetragonal), rutile (tetragonal) and brookite (orthorhombic). At room temperature, the direct gap energy  $E_g$  is 3.06 eV for rutile and 3.3 eV for anatase. These two values of the band gap allow a high absorption in the ultraviolet range. The anatase is formed at lower temperatures and sharing some properties with rutile such as hardness and density. At high temperature, around 800°C it will turn into rutile [6]. TiO<sub>2</sub> thin films have been prepared by many techniques such as reactive sputtering, sol gel [7], and chemical vapor deposition [8]. However, the sol gel technique attracts more attention by its low processing cost, simplicity and ability to produce a uniform thin film with a good



control in the preparation conditions. TiO<sub>2</sub> thin films are obtained using molecular precursors via inorganic polymerization reaction with titanium alkoxides [9]. The optical properties of the TiO<sub>2</sub> anatase films prepared by sol gel method deposited by spin coating are studied.

## 2. Experimental details

Nanocrystalline TiO<sub>2</sub> thin films are prepared using the sol-gel spin coating techniques. The sol was obtained by the partial hydrolysis and condensation of tetrabutyl orthotitanate Ti(OC<sub>4</sub>H<sub>9</sub>)<sub>4</sub> with H<sub>2</sub>O, the butanol and acetic acid used as solvent and catalyst. The procedure of preparation includes the dissolution of 1 mol titanium butoxide as precursor, 1 mol of H<sub>2</sub>O, 4 moles of butanol and 3 moles of acetic acid. After mixing the adequate proportions for 90 min, we obtain at the final a very transparent solution ready for the deposition. The gel was spin coated on the ITO substrate at 2500 rpm for 30 s for one and two coating. After, the film was dried at 100°C for 15 min and then heat treated at different temperatures ranging between 300°C and 600°C with increasing temperature rate of 5°C min<sup>-1</sup> for 2 h in a furnace.

The thin films have been systematically characterized after preparation and their eventual heat treatment. X-ray diffraction was used as a first characterization step to identify the structures of the crystallized phases present in the thin films. The diffractometer used was a Siemens D5005 Bragg–Brentano geometry (40KV, 20A) equipped with a copper anticathode wiring with CuK $\alpha$  radiation ( $\lambda=1.5406$  Å). The diffractograms were recorded at room temperature and the X-ray data were collected from 20° to 80° with a measurement time of 10 s. UV–visible spectroscopy studies were performed in order to determine the optical properties for wavelengths ranging from 250 to 2500 nm using a UV–visible-near infrared spectrometer PerkinElmer (Lambda-950) equipped with an integrating sphere.

## 3. Results and discussion

### 3.1. Structural properties

The XRD characterization of the annealed thin films obtained after one and two coating, were shown in figure 1(a, b). It can be seen that the diffraction pattern of TiO<sub>2</sub> annealed at 300°C does not exhibit a clear peaks and especially the peak around 25.35° is absent which indicates that the films are amorphous. However, from 400°C the intensity of the peaks around 25.35° was improved and they well detected, the diffraction pattern shows another small peak with a weak intensity characteristic of the anatase phase. At 500°C and 600°C, the peaks characteristic of anatase phase centered around 25.35° were defined revealing the nucleation and growth of grains. Using the JCPDS data, the peaks are well defined, there are 6 diffraction peaks showed at 25.35°, 37.56°, 41.45°, 44.48°, 45.45°, 55.72° and assigned (101), (004), (210), (200), (111), (211) planes respectively and correspond to anatase phase characterized by unit cell parameters ( $a=b=3.78$ ) and  $c = 9.516$ . Such a type of behavior has also been noticed by A.Ranjitha et al. [10] who used sol gel-dip coating for the deposition, they obtain anatase phase with high intensity peaks at 500°C.

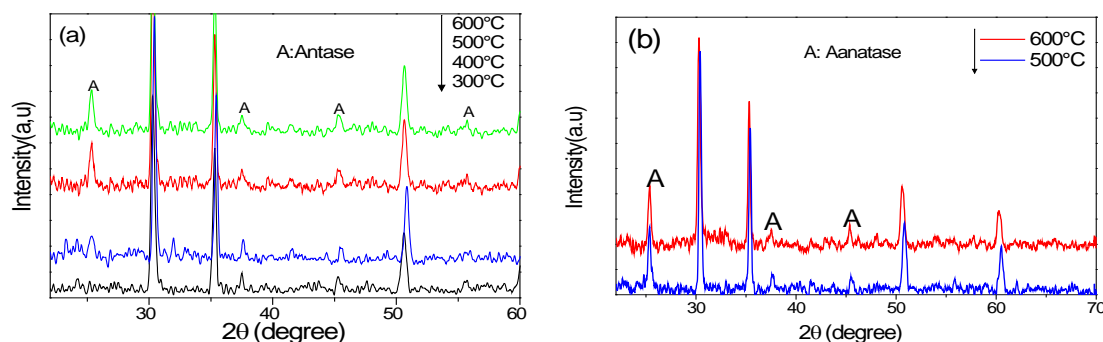


**Figure 1.** Evolution of diffraction patterns of the TiO<sub>2</sub> thin films after (a) one coating and (b) two coating for various annealing temperature. A=anatase.

As we raise the temperature of annealing, we observe an increase of the intensity correspond to the peaks which are centered around  $25.24^\circ$  characteristic of anatase phase. This late revealed an improvement of the crystalline structure. Also, it can be seen that the intensity of the peaks is very higher for films having two layers than one layer. This result is may be due not only to the improvement of the crystalline quality but also to the increase in proportion of titanium oxide and the density of layer. There is no peak corresponding to rutile phase which agrees with the literature showing that the films change their crystallinity nature from anatase to rutile when they annealed below  $600^\circ\text{C}$  [11]. The crystallite size of  $\text{TiO}_2$  thin films can be calculated from XRD patterns using Scherrer equation [12].

$$L = \frac{K\lambda}{\beta \cos \theta} \quad (1)$$

Where  $L$  is the crystallite size of  $\text{TiO}_2$  thin films,  $K$  is a constant equal to 0.94,  $\lambda$  is the wavelength of X-ray ( $\text{CuK}_\alpha = 1.5406 \text{ \AA}$ ) and  $\beta$  is the true half –peak width (FWHM). Table 1 shows the variation of the grains size for different annealing temperature and number of layers. As the temperature increases,  $\text{TiO}_2$  crystallites continue to develop and increase from 25.85 nm to 31.30 nm for two layers and from 10.72 nm to 20.97 nm for one layer. This results show that there was an improvement of the connections of Ti-O-Ti bond of the anatase phase as a function of the annealing temperature and the number of layer.

### 3.2. Optical characterizations

Figure 2 shows evolution of the optical transmittance spectra of the thin films of  $\text{TiO}_2$  (one, two layers) for various annealing temperature from  $300^\circ\text{C}$  to  $600^\circ\text{C}$ . All spectrums are characterized by the presence of two different regions: The first region of high transparency showing a few interference oscillations which are due to multiple reflections at the film/substrate and the film/air interfaces. The second region corresponds to strong absorptions characterized by a sharp drop in optical transmission. This abrupt drop, which is the fundamental absorption of thin layers, is due to the electronic transition between the valence and conduction bands of semiconductor materials.

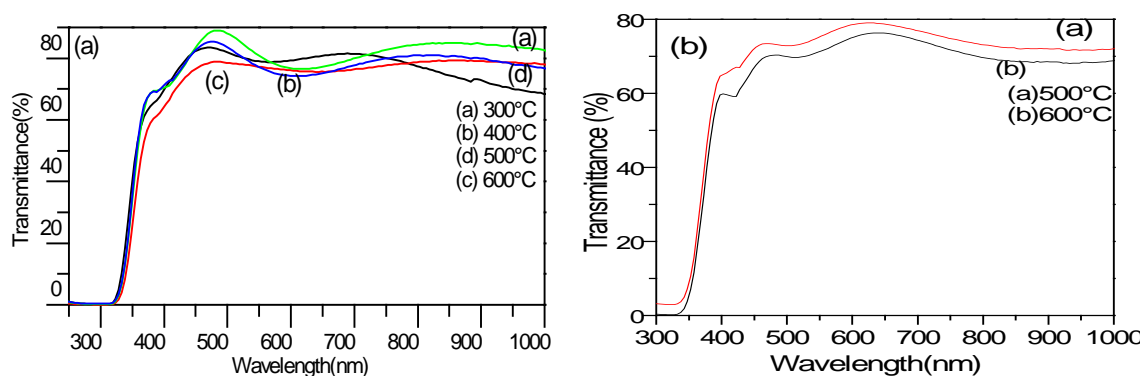


**Figure 2.** Optical transmittance spectra of  $\text{TiO}_2$  thin films at different annealing temperatures: (a) one layer, (b) two layers.

All the films obtained after one coating exhibit a transmittance higher than 80% in the visible region; they are highly transparent in the visible and opaque in the ultraviolet region. This high transparency is one of the properties that explain the interest of  $\text{TiO}_2$  thin films in solar cells applications. We find that the transmittance percentage of  $\text{TiO}_2$  thin films decreased slightly during annealing from  $300^\circ\text{C}$  to  $600^\circ\text{C}$ . This is due to the increase of the light diffusion with the crystallite size and particle aggregation. Thin films with one layer exhibit a higher transmittance than two layers. The increase in numbers of layers leads to a decrease in the transmittance percentage. The reflectance of all films

reaches over 20% in the visible region and it is clear that the thin film having one layer exhibits a reflectance higher than two layers.

**Table1.** Refractive index, porosity and thickness of TiO<sub>2</sub> thin films for different annealing temperatures.

Temperature (°C)	Eg (eV)		Porosity (%)		Refractive index		Thickness (nm)		L (nm)	
	One layer	Two layers	One layer	Two layers	One layer	Two layers	One layer	Two layers	One Layer	Two layers
<b>300</b>	3.92	-	40.03	-	2.05	-	70.36	-	8.84	-
<b>400</b>	3.87	-	30.28	-	2.17	-	65.69	-	10.72	-
<b>500</b>	3.80	3.64	28.82	42.40	2.19	2.02	60.67	95.40	18.09	25.85
<b>600</b>	3.74	3.50	15.01	32.68	2.35	2.14	61.66	94.67	20.97	31.30

The optical band gap energy was estimated using the Tauc's model [13]. Table 1 shows the energy gap values of TiO<sub>2</sub> thin films annealed at various temperatures. We observe that the gap energy of one layer decreases from 3.88 eV to 3.74 eV and from 3.64 eV to 3.5 eV for two layers with increasing annealing temperature. This decrease is due to the structural properties of the thin films. In fact, the annealing reduces the internal stresses and randomness formed during deposition and it affects the adjustment of relative position of atoms. The improvement in the crystallinity of the films and the decrease in the density of the grain boundaries with increasing the temperature affect very well the energy gap, this behavior has mentioned also by Ranjitha et al. [10].

### 3.3 Methods for calculating refractive index of thin films.

We used Heavens model to determine the thickness and the optical absorption energy gap coefficient of thin films, from analysis of their spectrum transmission  $T(\lambda)$  and reflectivity  $R(\lambda)$ . This model is particularly used in the field of low absorptions. To determine the thickness of the thin film, we must first calculate the refractive index  $n_c$ . The expression  $n_c$  of a weakly absorbent thin layer deposited on a transparent substrate was calculated from the measured UV-Vis reflectance spectrum in the region of a weakly absorbing film [14]:

$$n_c = \sqrt{n_s \times \frac{(1 + \sqrt{R_{\max}})}{(1 - \sqrt{R_{\max}})}} \quad (2)$$

Where  $n_s$  is the refractive index of the substrate and  $R_{\max}$  is the maximum average reflectance layer. The thickness  $d$  of the layer can then be deduced from the following relation:

$$d = \frac{m \times \lambda}{4 \times n_c} \quad (3)$$

Where  $m$  is the order of interference and  $\lambda$  is the wavelength. The porosity  $P$  of the thin films is calculated using the following equation [15]:

$$P = \left( 1 - \frac{n_c^2 - 1}{n_d^2 - 1} \right) \times 100(\%) \quad (4)$$

Where  $n_d$  is the refractive index of pore-free anatase (2.52) and  $n_c$  is the refractive index of the thin film. From table 1, it is clear that the refractive index of TiO<sub>2</sub> thin films increases with enhancing temperature treatment, contrary to the porosity which decreases. This is interpreted by the increase in the size of the grains and densification of the films and pore destruction in films during the increasing temperature treatment. In consequence the particles are electronically interconnected [16].

We see that variation of thin layers thickness depends on the temperature and it can be correlated with structural properties of thin film. Indeed, increasing temperature, the film becomes more crystallized and the grain size increases, therefore his compactness was enhanced and the film thickness decreases. The same observation was mentioned by Michiakh et al. [17]. Refractive index  $n(\lambda)$  of the layers as a function of wavelength  $\lambda$  was obtained from the transmission spectra in the weakly absorbing region of these films. We use the method of envelopes, it consists to draw two envelopes corresponding to the extrema of the interference fringes (an envelope for the maxima and minima for another transmission) and to take a value on each of these envelopes for the same wavelength  $\lambda$  rated  $T_{max}$  and  $T_{min}$  respectively. The refractive index  $n(\lambda)$  was given by:

$$n(\lambda) = \sqrt{s + \sqrt{s^2 - n_o^2(\lambda)n_s^2(\lambda)}} \quad (5)$$

Where  $n_o$  is the refractive index of air,  $n_s$  is the refractive index of substrate and  $s$  is determined by this expression:

$$s = \frac{1}{2(1+n_s^2)} + 2n \times \frac{T_{max}(\lambda) - T_{min}(\lambda)}{T_{max}(\lambda) \times T_{min}(\lambda)} \quad (6)$$

Figure 3 shows the spectral variation of the refractive indices  $n(\lambda)$  of the thin films (one and two layers) of TiO<sub>2</sub> for 500°C and 600°C. We note that for the low wavelengths,  $n(\lambda)$  reaches a maximum for a value  $\lambda_m$  and it shifts to longer wavelengths by increasing the annealing temperature. In the area of transparency,  $n(\lambda)$  stabilizes and tends to be constant. This maximum  $\lambda_m$  is interpreted as the energy corresponding to the optical gap of the thin layer. The optical gap energy of the layers decreases with the annealing temperature therefore  $n(\lambda)$  increases from 2.09 to 2.11 and from 2.17 to 2.18 for one and two layers respectively.

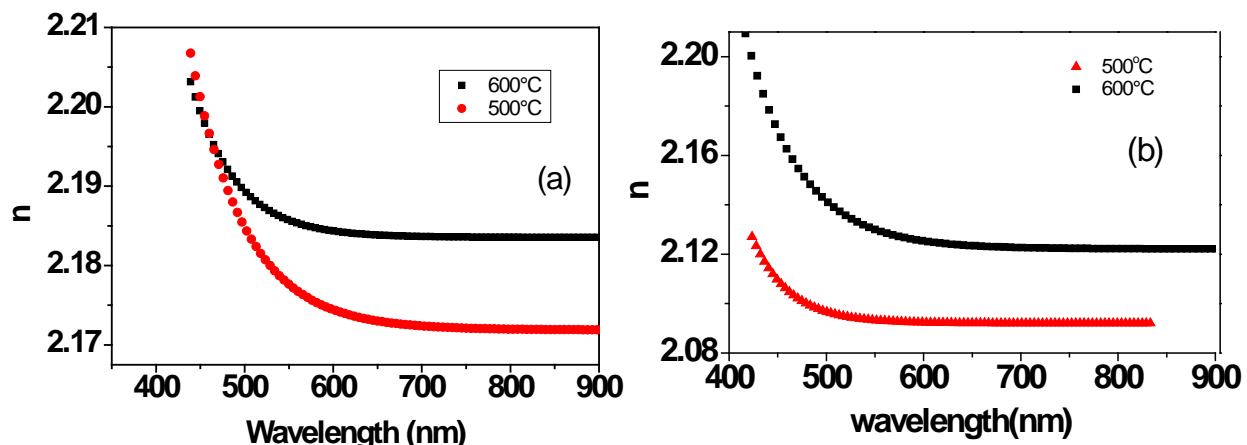


**Figure 3.** Refractive index as a function of wavelength of TiO<sub>2</sub> films: (a) two layers, (b) one layer.

Present values of refractive index are slightly lower than the reported values in anatase single crystal (2.50). It could be due to partial crystallinity and low atom mobility of the films at room temperature. It has been noticed that the refractive index and band gap energy show opposite trends with annealing. Such a type of behavior has also been reported by Khan et al. [18].

#### 4. Conclusion

We have prepared nanocrystalline TiO<sub>2</sub> thin films deposited on ITO substrates using tetrabutyl-orthotitanate precursor by employing a simple and inexpensive sol-gel spin coating technique. We have observed that films crystallize in the anatase phase after annealing at 400°C and the grain size showed depends on annealing temperature indicating recrystallization. Band gap of the film decreased from 3.92 eV to 3.74 eV for one layer and from 3.65 eV to 3.5 eV for two layers when the temperature varied from 300°C to 600°C. The as deposited films were porous and were found to become dense as annealing temperature increases. We observe an increase in refractive index with the temperature annealing, contrary to the band gap energy which decreases. Annealing has been found to have a strong influence on structural and optical properties of nanocrystalline TiO<sub>2</sub> thin films.

#### References

- [1] Jin P, Miao L, Tanemura S, Xu G, Tazawa M, Yoshimura K 2003 *Appl. Surf. Sci.* **212–213**, 775–781.
- [2] Ko H H et al., 2012 *Int. J. Mol. Sci.* **13**, 1658–1669.
- [3] Huang L, Liu T, Zheng H, Guo W, Zeng W 2012 *J. Mater. Sci: Mater. Electron* **23**, 2024–2029.
- [4] Xu Z, Manhong L, Yongfa Z 2007 *Thin Solid Films* **515**, 7127–7134.
- [5] Torchani A, Gharbi R and Fathallah M 2014 *Sensors & Transducers*, **27**, 185-189.
- [6] Afuyonia M, Nashed G, Nasser I M 2011 *Energy Procedia* **6**, 11–20
- [7] Brinker C J, Harrington M S 1981 *Solar Energy Mater*, **5**, 159 -172.
- [8] Bessergenev V G et al. 2002 *Vacuum* **64**, 275–279.
- [9] Biju K P, Jain M K 2008 *Thin Solid Films* **516**, 2175-2180.
- [10] Ranjitha A, Muthukumarasamy N, Thambidurai M, Balasun Daraprabhu R, Agilan S 2013 *Optik* **124**, 6201– 6204.
- [11] Sugapriya S, Sriram R, Lakshmi S 2013 *Optik* **124**, 4971– 4975.
- [12] Cullity B D 1978, *Elements of X-ray Diffraction*, Wesley, second ed Addison.
- [13] Calderon-Moreno J M et al. 2014 *Ceramics International* **40**, 2209–2220.
- [14] Vasanthkumar C V R, Mansingh A 1990, in Seventh IEE International symposium on Application of Ferroelectrics, *IEE*, New York **713**.
- [15] Moss T S 1961 *Optical Properties of Semiconductors*, Butterworths, Sci. Pub. Ltd, London.
- [16] Mathews N R et al. 2009 *Solar Energy* **83**, 1499–1508.
- [17] Mechiakh R, Ben Sedrine N, Chtourou R 2011 *Applied Surface Science* **257**, 9103-9109.
- [18] Khan A F et al. 2014 *Material Science in Semiconductor Processing* **2**, 1369-8001.